ANNALI DI GEOFISICA, VOL. 41, N. 3, August 1998

Boundaries of magnetic anomaly sources in the Tyrrhenian region

Federico Cella, Maurizio Fedi, Giovanni Florio and Antonio Rapolla
Dipartimento di Geofisica e Vulcanologia, Università di Napoli «Federico II», Napoli, Italy

Abstract
Analysis of the analytic signal of the aeromagnetic field in the Tyrrhenian region allowed the systematic location of the boundaries of magnetic shallow sources. This method was chosen because of its independence from the magnetization and inducing field direction, and the results were similar to those of the boundary analysis of the horizontal gradient of the pseudogravity transformed field. The analytic signal was computed by a stable algorithm based on the second order horizontal derivatives of the field and Laplace equation. The complexity of the investigated area is well reflected in the aeromagnetic field and an objective and systematic study, such as boundary analysis, provided a rather complete description of the main regional structures. Significant trends indicated the existence of structures, whose nature was still unknown or uncertain. These included structures located between the Vavilov and De Marchi seamounts, NW of Stromboli Island, south of Ponza Island, a buried horst immediately south of the Cilento coastline, a body located northwest of the Cassinis seamount and other small magnetized structures located south of the Tuscanian archipelago. In many cases, a better definition of several structures previously recognized was obtained as in the case of some tectonic alignments (*e.g.*, the Elba ridge, the Romolo and Selli lines, etc.), a large number of igneous seamounts (*e.g.*, Magnaghi, Marsili, Vavilov, Anchise, Quirra, Enarete, Eolo and Sisifo seamounts) and several crystalline outcrops (*e.g.*, Ichnusa, Vercelli, M. della Rondine, Tiberino, Cassinis, Traiano, Glauco and Augusto seamounts).

Key words *magnetic anomalies – crust structures – Tyrrhenian basin – Italy*

1. The magnetic field of the Tyrrhenian region

The Tyrrhenian basin is a small deep asymmetric basin, partially floored with basaltic crust. Its northern sector is composed of orogenic continental crust that underwent an intense anatectic magmatism of the Upper Miocene age (Barbieri *et al.*, 1986), followed by cyclic extensional phases (Bernini *et al.*, 1990). In the western part of the basin the continental crust was stretched and thinned by rotational normal faulting prior to the formation of the basaltic crust (Moussat *et al.*, 1985), with the formation of asymmetric, tilted basement blocks (Kastens *et al.*, 1988). The southwestern part of the Tyrrhenian basin (Sardinia channel) is formed by thinned continental crust, underplated by partial melt in the central region (Peirce and Barton, 1992). The central-eastern part of the basin is the youngest and the deepest and mainly composed of large extensions of tholeiitic basalts, including several alkali basalt volcanic centers (Magnaghi, Vavilov, Marsili), located within a strongly stretched ancient continental crust (Kastens *et al.*, 1988).

Mailing address: Dr. Maurizio Fedi, Dipartimento di Geofisica e Vulcanologia, Università di Napoli «Federico II», Largo S. Marcellino 10, 80138 Napoli, Italy; e-mail: fedi@axposf.dgv.unina.it

Several models were suggested to describe the geodynamical evolution of the basin. One of the most supported models interprets the Tyrrhenian basin as a back-arc basin (Finetti and Del Ben, 1986; Malinverno and Ryan, 1986; Patacca *et al.*, 1990)

Locardi and Nicolich (1988) suggest an alternative model explaining the magmatic setting in the perityrrhenian regions not by the hypothesis of a westward dipping subduction below the Central and Southern Apennines but by the presence of a fluidized asthenospheric mass which flowed from the top of the Tyrrhenian asthenolith toward the Appenninic belt.

A third model hypothesizes a progressive south-eastward migration of the spreading centre of the Tyrrhenian basin, substantially confirmed and explained by recognising a different subduction hinge «rollback» rate of a variously dense and thick Adriatic lithosphere, due to an eastward oriented push of the asthenosphere acting on the slab at depth. To describe this mechanism, the global westward motion of the lithosphere relative to the asthenosphere, has to be taken into account (Doglioni, 1991; Doglioni and Flores, 1995)

The aeromagnetic field of the Tyrrhenian Region shows the presence of a complex set of many anomalies located in correspondence of volcanic islands, seamounts, tectonic lineaments and morphological highs around the batial plain border. Most anomalies present a high amplitude (from 200 to 1200 nT for the Vavilov, Magnaghi, Marsili and Palinuro seamounts) and are strictly related to the recent geodynamic evolution of this area.

Many lower amplitude and high frequency anomalies (up to 30 nT) indicate the presence of many structures of various origin, nature and age, so indicating the very complex evolution of this basin (Morelli, 1982). Moreover, some weak and low-frequency anomalies characterize the Sardinian basin, the Tyrrhenian shelf of the Sicilian and the Calabro-Campanian offshore. Selli (1981) pointed out various transform faults by observing magnetic anomalies, volcano alignments and tectonic lineaments. A SE-NW total magnetization direction (ranging from $-30°$ to $-50°$) was argued for several anomalies located around the batial plain (Fedi and Rapolla, 1988). It has been interpreted as due to the complex and multiphase rotational movements accompanying the Tyrrhenian opening, in good agreement with the anticlockwise movements suggested for the Southern Apennines on the basis of independent evidence (Finetti and Del Ben, 1986; Incoronato and Nardi, 1989).

Due to such a structural and dynamic complexity, the aeromagnetic field is expected to yield a very meaningful description of the Tyrrhenian area. Hence, processing the aeromagnetic field by rather objective techniques, such as boundary analysis, may be used to obtain a systematic and rather complete description of the regional structural setting.

2. Techniques of boundary analysis

The horizontal location of the lateral edges of source-bodies of potential field anomalies can help detection of contacts between structures with different density and/or magnetization, *e.g.*, lateral boundaries of plutons in sedimentary cover, volcanic bodies, dykes and laccolites.

Since the '70s, several methods have been proposed to automatically define the source parameters of gravity and magnetic anomalies. These parameters are essentially the boundary location and the depth of the density/magnetization anomaly sources. The success of these techniques is based on the possibility to obtain quantitative solutions with few assumptions and with a better resolution than from the original potential field data. This is mainly true as far as magnetic fields are concerned, because of difficulties in the visual identification of source edges at non-polar magnetic latitudes.

The information related to the boundaries of the sources may be enhanced by either of two techniques based on the horizontal and vertical derivatives of the potential field: horizontal gradient analysis and analytic signal analysis.

The most simple method concerns the calculation of the horizontal derivative (Cordell, 1979; Cordell and Grauch, 1985) of the poten-

tial field (M):

$$h(x, y) = \sqrt{\left[\left(\frac{\partial M}{\partial x}\right)^2 + \left(\frac{\partial M}{\partial y}\right)^2\right]}.$$

In the case of gravity anomalies, sources vertically sloping have derivative maxima located along their boundaries.

In the case of magnetic data, anomalies appear displaced with respect to their sources, unless at poles. This leads to mislocating the source boundaries. Reduction to the pole or pseudogravity transformations (Baranov, 1975; Fedi, 1990) may correct for this effect, but the directions of the inducing field and of the average magnetization vectors need to be known. In this regard, pseudo-gravity integration appears more suitable than reduction to the pole, since it is less dependent upon the actual direction of the magnetic field and the average source magnetization. Moreover, it is a smoothing operator so that the horizontal derivation of the pseudogravity field is more stable than that for the reduced to the pole field. Nevertheless, in both cases, a constant direction is assumed for the magnetization vector, while it is generally not homogeneously directed over the map. Hence, several transformations should be needed to obtain meaningful information from the horizontal derivative data, each one relative to a different direction of the magnetization vector.

As an alternative technique for finding source boundaries, we considered the analysis of the analytic signal (Nabighian, 1984), a complex quantity whose real and imaginary parts are respectively the horizontal and vertical derivatives. The amplitude function of the analytic signal (Roest *et al.*, 1992) is then given by the vectorial sum of the three derivatives of the potential field M:

$$|A(x, y)| = \sqrt{\left[\left(\frac{\partial M}{\partial x}\right)^2 + \left(\frac{\partial M}{\partial y}\right)^2 + \left(\frac{\partial M}{\partial z}\right)^2\right]}.$$

As in the case of the horizontal derivative, the position of the maxima estimated by the analytic signal is located along the boundaries of the anomaly source, provided the discontinuities are near vertical. Several tests performed on gravity data (fig. 1a-d) evidenced that lateral dimensions of prismatic source bodies as resulting from analytic signal are slightly underestimated with respect to the real ones, whereas this drawback is not present when the horizontal gradient is used. The same considerations are easily extended to the magnetic case. However, in this case, the analytic signal presents the significant advantage that its shape does not depend upon the directions of the inducing field and of the magnetization vector. So, to perform boundary analysis using the analytic signal, there is no need to previously reduce magnetic anomalies to a polar latitude.

The final step of boundary analysis concerns recognizing the maxima of the analytic signal (or of horizontal field derivative) to define the lateral boundaries of the sources. This operation was made by means of an automatic technique proposed by Blakely and Simpson (1986). This method finds the maxima comparing the value of each intersection of grid data with its nearest neighbours in four directions, along the row, column, and both diagonals. This comparison is made by testing the following inequalities:

$$M_{i-1,j} < M_{i,j} > M_{i+1,j}$$

$$M_{i,j-1} < M_{i,j} > M_{i,j+1}$$

$$M_{i+1,j-1} < M_{i,j} > M_{i-1,j+1}$$

$$M_{i-1,j-1} < M_{i,j} > M_{i+1,j+1}$$

where M stands for horizontal derivative of pseudogravity, gravity or for analytic signal anomaly. For each inequality satisfied, a counter N (significance level) is increased, ranging from 0 to 4, so defining the «quality» of the maximum. The horizontal location and the amplitude of each maximum are finally calculated by interpolation of a second order polynomial.

To obtain the analytic signal, the calculation of the vertical derivative is needed, in addition to the horizontal one. There are several meth-

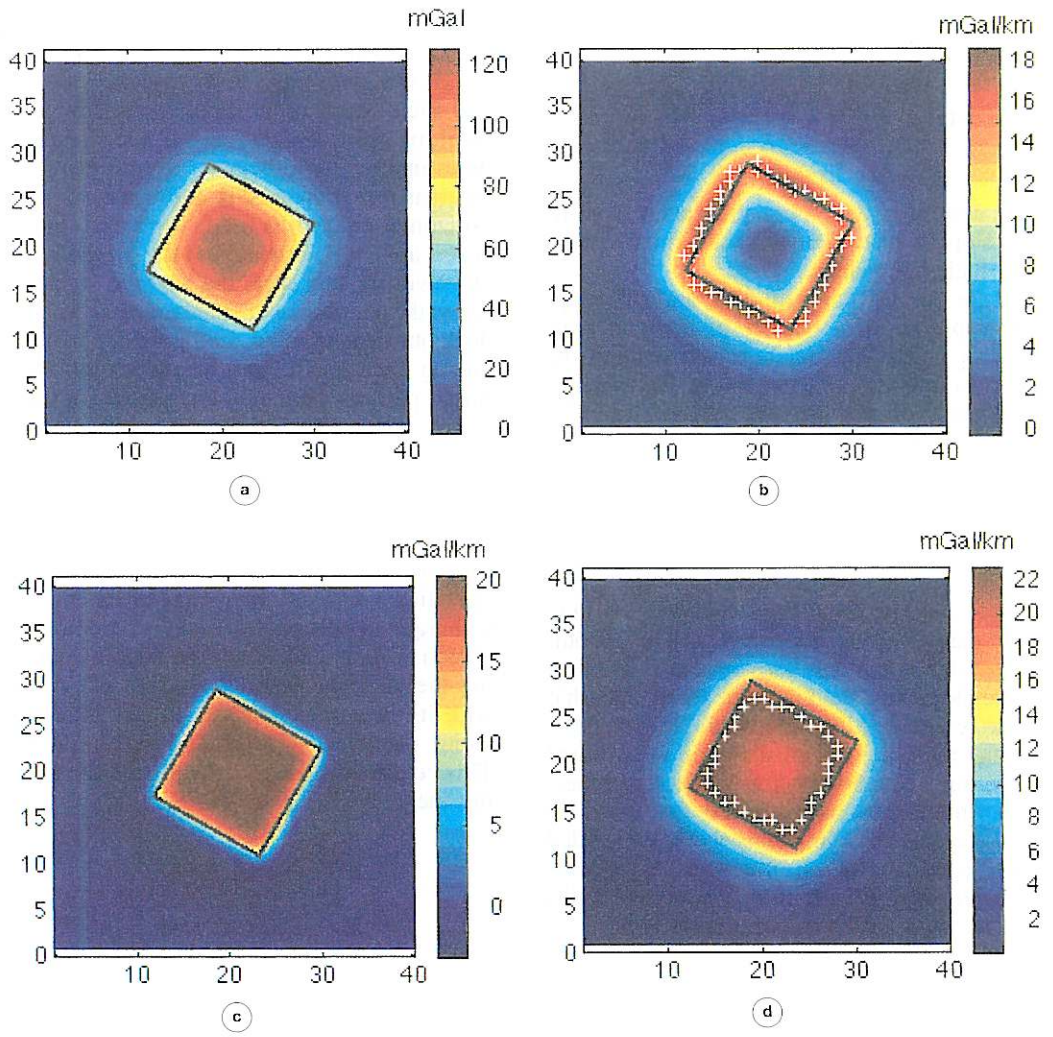

Fig. 1a-d. a) Synthetic error-free gravity (or pseudogravity) field generated by a square based prismatic body with the following features: width = 14 km; depth to the top = 1.2 km; thickness = 5 km; $\Delta\rho$ = 1 g/cmc. b) Horizontal gradient. c) Vertical gradient (analytically computed). d) Analytic signal.

ods to compute the vertical derivative, but they are not equally stable when used in real cases. We performed several tests on gravity anomalies which obviously extend to the pseudogravity anomalies in the magnetic case. They show that the convolution of the measured field with a vertical differentiation operator provides good results only for a very high signal to noise ratio. In fact, a boundary analysis of potential fields generated by a synthetic source-body and affected by small gaussian random errors (3% of anomaly amplitude) provides

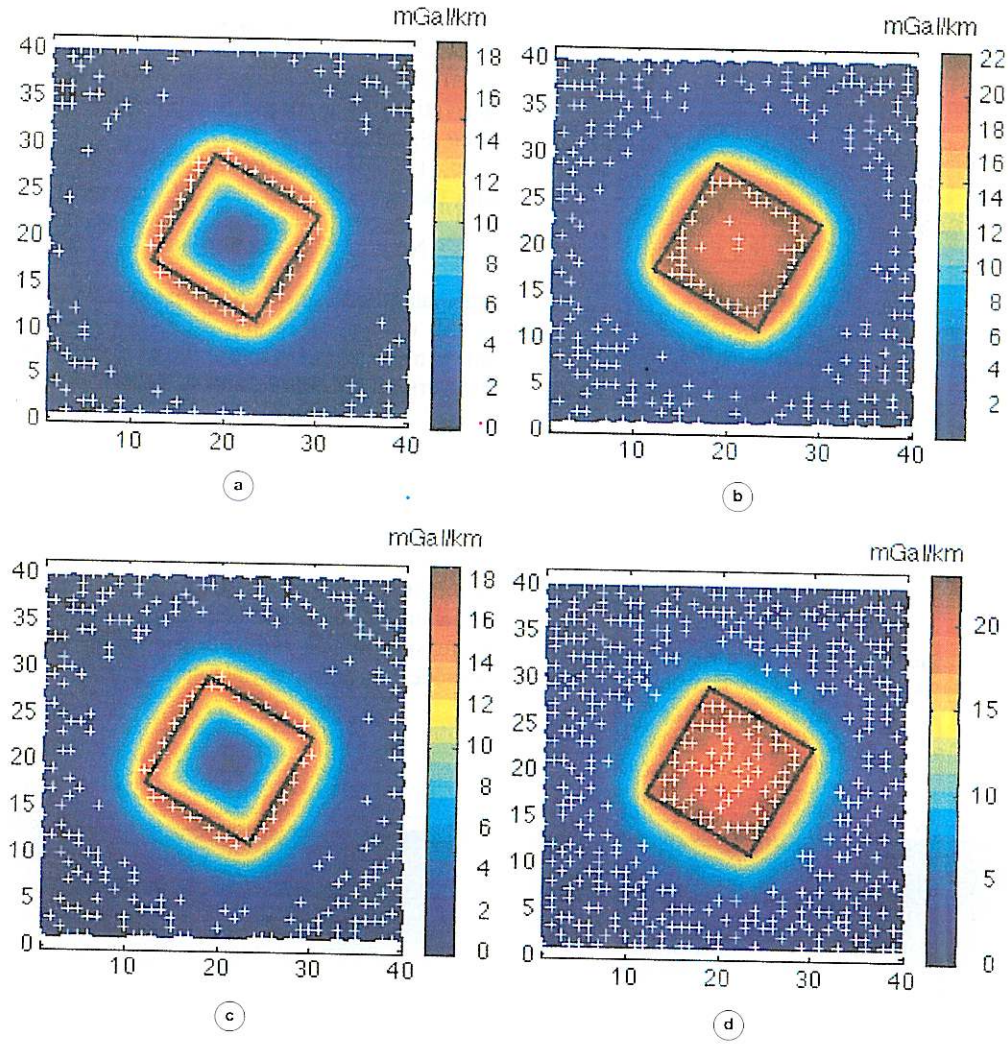

Fig. 2a-d. Boundary analysis of a synthetic gravity field (same of fig. 1a) affected by gaussian random errors with amplitude equal to 3% and 10% of the original anomaly. a) Horizontal gradient (error = 3%). b) Analytic signal. Vertical derivative was obtained by numerical convolution (error = 3%). c) Horizontal gradient (error = 10%). d) Analytic signal. Vertical derivative was obtained by numerical convolution (error = 10%).

poor results. When the error increases (10%) the edge location becomes totally unreliable (fig. 2a-d).

In order to compute a more stable vertical derivative, given a potential field M, a different technique was here used (we call it Integrated Second Vertical Derivative, ISVD), based on the Laplace equation formula:

$$\frac{\partial^2 M}{\partial z^2} = -\frac{\partial^2 M}{\partial x^2} - \frac{\partial^2 M}{\partial y^2}. \qquad (2.1)$$

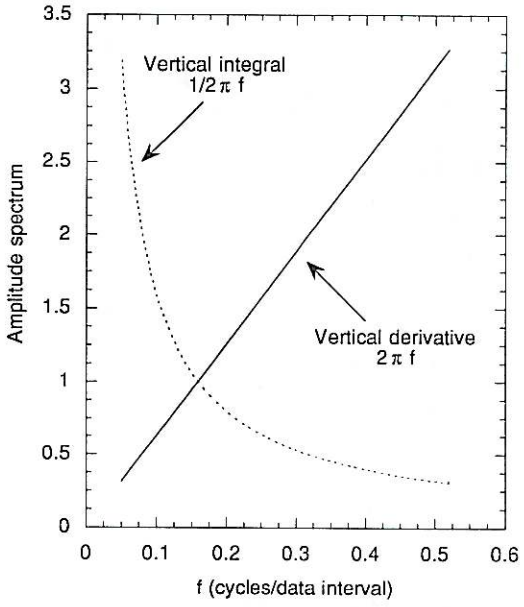

Fig. 3. Frequency response of the vertical integral operator compared to the vertical derivative operator.

It consists in computing the first order vertical derivative of M by:

a) Calculating its second order horizontal derivatives by a simple five-point finite difference algorithm.

b) Using Laplace equation (eq. (2.1)) to obtain the second order vertical derivative.

c) Numerically convolving $\frac{\partial_2 M}{\partial z^2}$ with the smoothing operator of vertical integration (fig. 3).

As evidenced in fig. 4a,b, this method is much more stable than the direct calculation of the vertical derivative and it should work well in real noisy cases.

It must be recalled that both these methods assume vertical and abrupt contrasts. Otherwise, the boundaries detected will be shifted toward the dip direction of the discontinuity, in a measure depending on their inclination and depth (Grauch and Cordell, 1987). This effect is generally small and becomes negligible with increasing lateral widths of the source or when considering regional data sets.

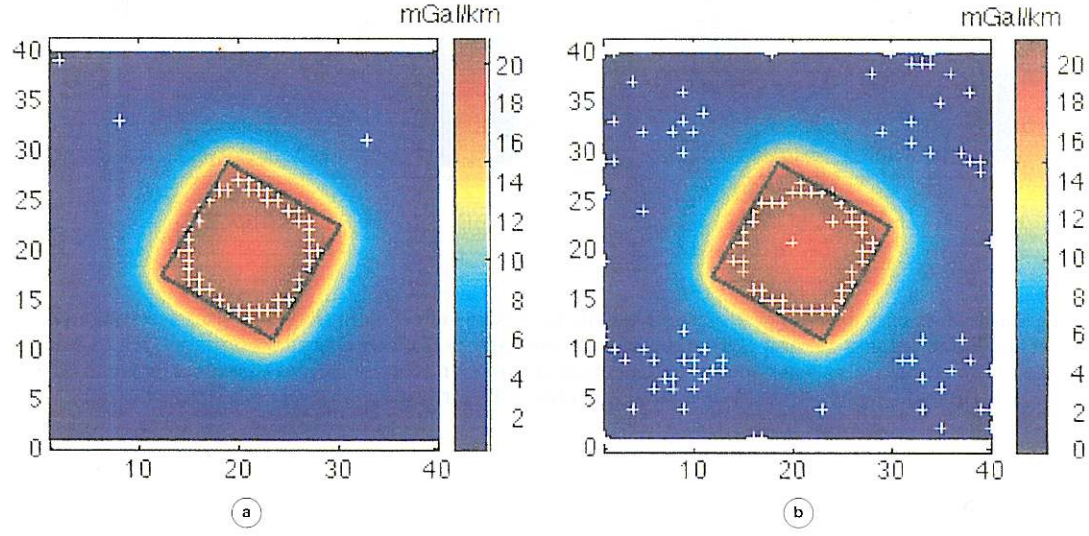

Fig. 4a,b. Boundary analysis of the same field of fig. 1a, but affected by gaussian random errors with amplitude equal to 3% and 10% of the original anomaly. a) Analytic signal. Vertical derivative was obtained by vertical integration (see text; error = 3%). b) Analytic signal. Vertical derivative was obtained by vertical integration (see text; error = 10%).

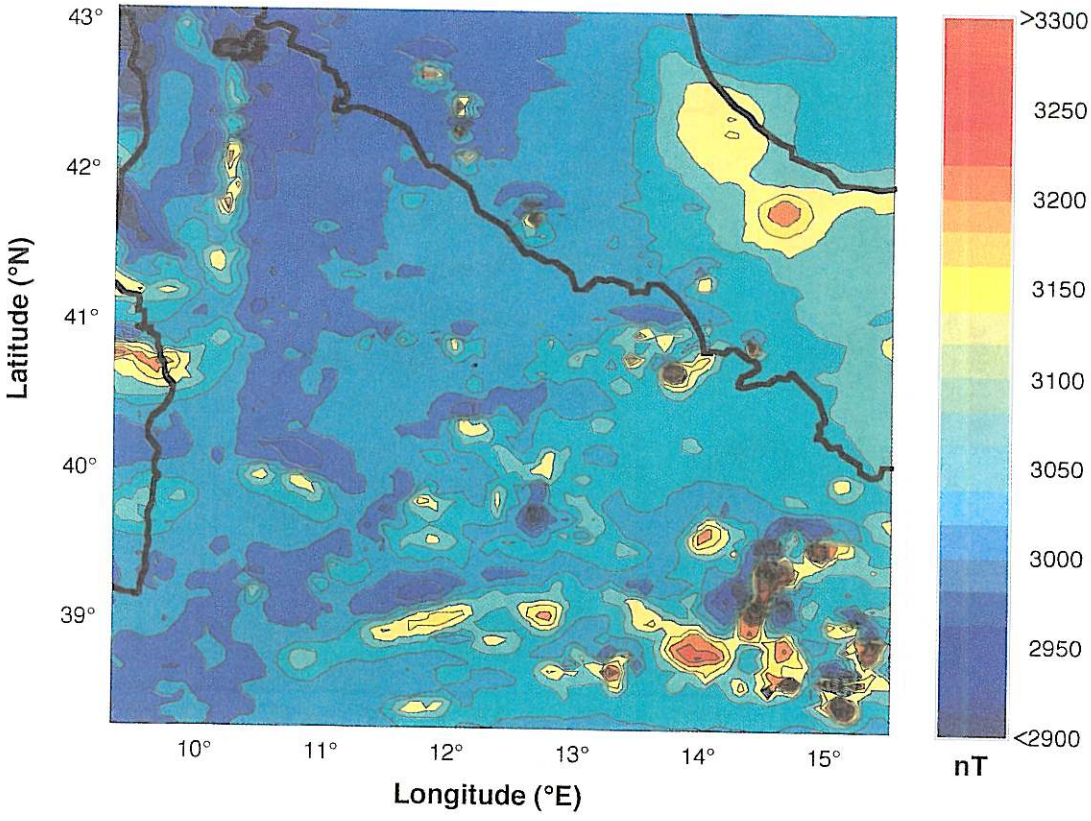

Fig. 5. «Residual Magnetic Anomaly Map of Italy» (AGIP, 1981). The data set consists in a 90×90 grid with 6 km step.

3. Data analysis and interpretation

The analysis regarded the whole Tyrrhenian basin, covering an area whose coordinates range from 38°30′ to 42°50′ Lat. N and from 9°23′ to 15°33′ Long. E (fig. 5). It was based on a 90×90 data set at a 6 km step, windowed from the «Residual Magnetic Anomaly Map of Italy» (1:500 000) published by AGIP (1981).

A careful study of the boundary analysis from horizontal derivatives was first conducted. Slight but often significant differences in the location of the maxima were observed as the magnetization vector direction was varied to make the pseudogravity transformation. The analytic signal was therefore preferred, due to its substantial independence from the magnetization vector direction.

From a preliminary analysis, the found edges disclosed some structures already described by the magnetic field itself. Nevertheless, the boundary analysis yielded additional information about the lateral extent of the source bodies. Furthermore, the transformation of the magnetic field to the analytic signal enhances the low amplitude anomalies and provides a better resolution for close anomalies. Finally, the amplitude of the analytic signal may be used to have some indications on the nature of the source bodies. In fact, as a first approximation, volcanic or basic igneous rocks should

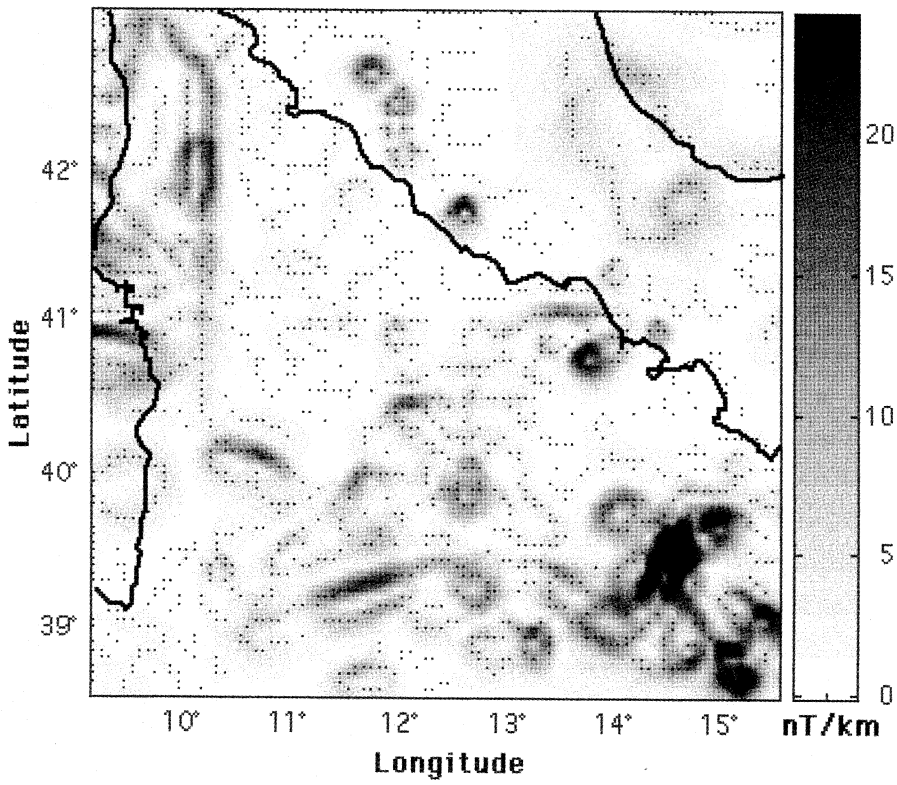

Fig. 6. Analytic signal of the magnetic field shown in fig. 5. Black points represent the position of the maximum amplitude values of the analytic signal.

have higher values of the analytic signal than felsic crystalline rocks.

The analysis revealed few linear trends and, on the contrary, indicated the prevailing presence of sources correlable to igneous bodies, volcanoes, outcropping fragments of crystalline basement, etc. This is not surprising, since several tectonic lines (dip-slip faults, transcurrent and transtensive faults) are zones of crustal weakness and therefore represent preferential pathways of magma rising or areas of basement outcropping. Thus, many tectonic lines may just be identified by alignments of volcanic bodies or continental horsts.

Two main kinds of source edges are shown by the maxima trends on the analytic signal map (fig. 6):

– Boundaries well correlated with known structural features (fig. 7).

– Boundaries partially or not correlated with known structural features (fig. 8).

3.1. *Boundaries well correlated with known structural features*

The presence of many features already inferred from previous studies (*e.g.*, Finetti and Del Ben, 1986; Barberi *et al.*, 1991) is clearly evidenced by the edge analysis, but the analysis points out new insights about their nature and extent.

For instance, our analysis shows an offshore enlargement of magnetic structures along

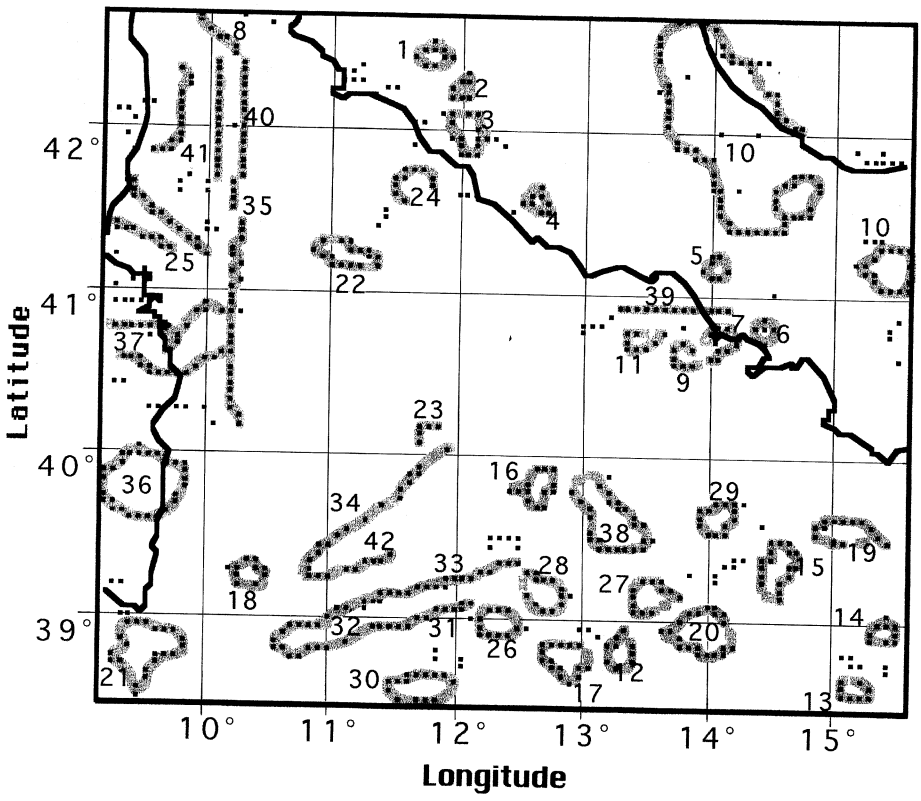

Fig. 7. Location of the main trends of analytic signal maxima evidencing structures already recognised in previous studies. Identified structures and corresponding numbers are listed in table I.

the eastern coast of Sardinia, disclosed by two broad and circular maxima edges. It may be correlated to outcropping metamorphites and acid plutonites, as in their on-shore part.

The presence of deep magnetic sources located along the eastern margin of the Apenninic chain is also evident; the origin of these magnetized bodies is probably linked to the genesis of the Apennines (Florio, 1993).

Further on the northern edges of the Tyrrhenian basin, circular trends of maxima emphasise the presence of the main onshore volcanic centers of the Italian peri-Tyrrhenian belt (Bolsena, Vico, Bracciano, Albano, Roccamonfina, Vesuvius and Phlegraean Fields). A similar correspondence exists as far as some peri-Tyrrhenian islands are concerned (Elba, Ischia, Ventotene, Ustica, Panarea and Stromboli). Within the Tyrrhenian basin the boundary analysis disclosed significant trends around some major submarine volcanoes of the abyssal plain, with prevailing tholeiitic basalts (Marsili and Vavilov seamounts). Moreover, the edges of many secondary seamounts were also clearly revealed. Some of them are volcanic centers characterized by a magmatism ranging from alkaline or calc-alkaline to shoshonitic and are located around the edges of the abyssal plain (Palinuro, Anchise, Quirra, Enarete, Eolo and Sisifo seamounts).

Other seamounts located around the batial plain, which are fragments of continental margins locally occurring with magmatic effusions, were also evidenced by our analysis.

They included the Ichnusa, Vercelli, M. della Rondine (*cf.*, Barberi *et al.*, 1991), Tiberino, Cassinis, Traiano, Glauco and Augusto (with a small lateral volcanic center) seamounts. Some of the structures outlined in these areas may also be linked to buried sources and only partially related to the topographic relief. The Marsili Smt. structure is instead related to a couple of magnetic anomalies, possibly owing to a polyphasic evolution of this volcano. Our analysis showed instead a number of analytic signal maxima entirely surrounding the seamount.

In some cases, near-structures appeared enclosed in a unique circular trend of maxima, such as the Eolo, Sisifo and Enarete submarine volcanoes. This effect depends on the regional type of data used.

A significant correspondence seems to occur between trends of maxima and some other reliefs like the Poseidone Smt. (with probably associated Issel Smt., Barberi *et al.*, 1991), where a not sampled acoustic basement outcrops. This is also the case of the Aceste Smt. (*cf.*, Barberi *et al.*, 1991; named Tiberio Smt. in Finetti and Del Ben, 1986) with a close eastward-located small relief, that were both interpreted as probable volcanic structures (Barberi *et al.*, 1991). They are delimited by a unique circular trend of maxima.

As far as linear trends of maxima are concerned, two alignments are easily recognizable in the analytic signal map. They coincide with the southern and northern boundaries of two seamounts (Pompeo and Giulio Cesare sea-

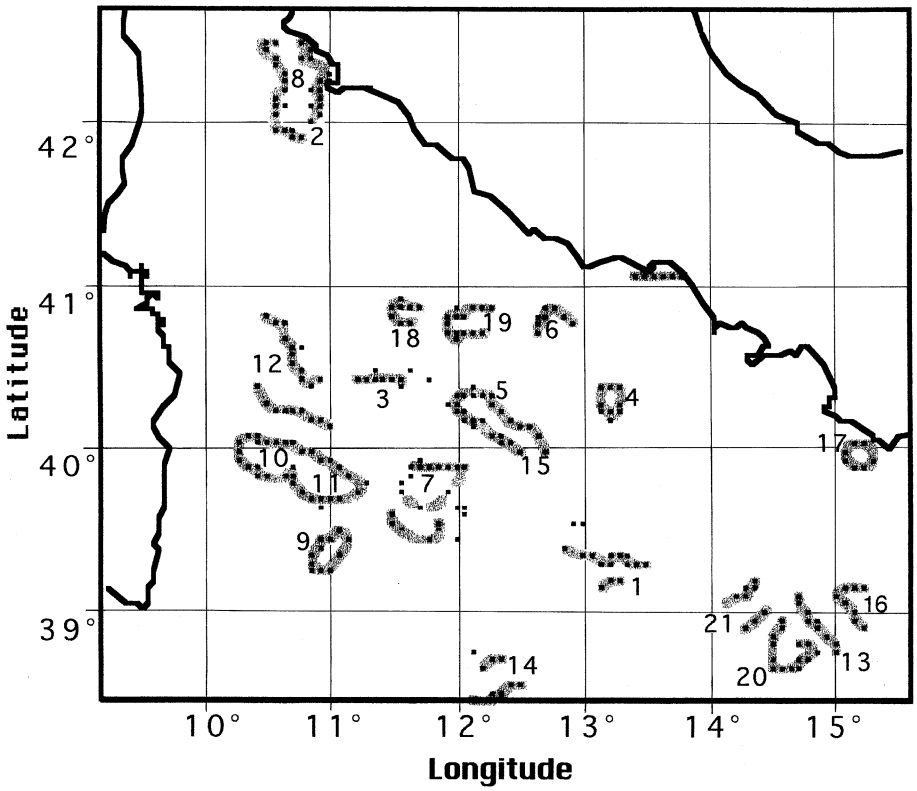

Fig. 8. Location of the main trends of analytic signal maxima evidencing structures partially or not correlated with known structural features. Identified structures and corresponding numbers are listed in table II.

Table I. Boundaries well correlated with known structural features

1 – Bolsena volcano
2 – Vico volcano
3 – Bracciano volcano
4 – Albano volcano
5 – Roccamonfina volcano
6 – Somma-Vesuvius volcano
7 – Phlegraean Fields
8 – Elba Island
9 – Ischia Island
10 – Deep magnetic sources probably linked to the genesis of Apennines (Florio, 1993)
11 – Ventotene Island
12 – Ustica Island
13 – Panarea Island
14 – Stromboli Island
15 – Marsili Smt.
16 – Vavilov Smt.
17 – Anchise Smt.
18 – Quirra Smt.
19 – Palinuro Smt
20 – Sisifo Smt.
21 – Ichnusa Smt.
22 – Vercelli Smt.
23 – M. della Rondine (Selli ridge)
24 – Tiberino Smt.
25 – Southeastern offshore prolongation of the tectonic contact between the Alpine units on Corsican foreland.
26 – Traiano Smt.
27 – Glauco Smt.
28 – Augusto Smt.
29 – Poseidone Smt.
30 – Aceste Smt. (Tiberio)
31 – Pompeo Smt.
32 – Giulio Cesare Smt.
33 – Romolo magnetic line
34 – Selli Line
35 – Etruschi mounts
36 – Outcropping metamorphites and acid plutonites (central side of the Eastern Sardinian coastline)
37 – Outcropping metamorphites and acid plutonites (northern side of the Eastern Sardinian coastline)
38 – Issel basin
39 – Ponza fault
40 – Elba ridge
41 – Corsica basin
42 – Structural line corresponding to the southern edge of the Giulio Cesare oceanized basin.

mounts) aligned in WSW-ENE direction. The southern one was interpreted as a reverse fault southward dipping and delimiting a volcanic thrust block (Finetti and Del Ben, 1986). The northern alignment seems to coincide with the Romolo magnetic line (Finetti and Del Ben, 1986), interpreted as a left transcurrent fault delimiting southward the area with thin oceanic crust in the Tyrrhenian Sea and marked by the presence of igneous bodies and basement uplifts (Finetti and Del Ben, 1986).

A tectonic line that played a significant role in the opening of the Tyrrhenian basin, the Selli line, is easily identified by boundary analysis. It probably represents a normal fault westward delimiting the area with thin oceanic crust in the Tyrrhenian Sea (Finetti and Del Ben, 1986). Another structural line corresponding to the southern edge of the Giulio Cesare (Finetti and Del Ben, 1986) oceanized basin is also clearly recognised.

Northwestward, the analysis of maxima allowed a set of tectonic lines to be clearly recognized; these tectonic lines are N-S aligned and delimit the Corsica basin and the Elba ridge. One of them is very marked and its southward prolongation outlines the Etruschi Mounts and the Baronie ridge on their west side. This linear trend stops abruptly in correspondence with the NW-SE aligned Asinara right transcurrent fault. Northward, it continues up to Elba Island. Some other minor faults can be evidenced by the boundary analysis, even if less clearly. This is the case of the Ponza fault.

The presence of a significant trend delimiting an area without relevant magnetic anomalies can be noted. It corresponds to the Issel basin, located in the abyssal plain, between the Marsili and Vavilov volcanoes.

3.2. *Boundaries partially or not correlated with known structural features*

Several edges seem to be partially or not at all related to structural features identified by most studies on the Tyrrhenian basin (*e.g.*, Finetti and Del Ben, 1986; Barberi *et al.*, 1991). In many cases, this reflects the high significance of the magnetic field description for the complex structures occurring in areas of intense geodynamics. For example, the analytic signal anomaly of the Magnaghi Smt. is not completely correlated with the topography and includes also a more southern area. Moreover, the western edge of the structure seems to be more magnetic than the rest. Such a distribution of magnetization reveals a great complexity in volcano formation, as already pointed out by Fedi *et al.* (1994).

Table II. Boundaries partially or not correlated with known structural features.

1	Orazio and Lucrezio seamounts
2	Body located south of the Giglio Island
3	Secchi Smt.
4	Albatros Smt.
5	De Marchi Smt.
6	Probable igneous buried body south of Ponza Island
7	Magnaghi Smt.
8	Giglio Islands and Formiche di Grosseto reef
9	Two bodies, with coordinates 10°55′ Long. E and 39°20′ Lat. N
10	Cornaglia Smt. and other small seamount
11	Mayor and Sallustio Smts.
12	Baronie ridge
13	Vulcano fault
14	Drepano Smt.
15	Area between Vavilov and De Marchi Smts. (Gortani ridge)
16	Area north-west of Stromboli Island
17	Horst buried below young sediments
18	Bathymetrical high including Cassinis Smt. and an outcrop of acoustic basement
19	Body with coordinates 12°5′ Long. E and 40°50′ Lat. N.
20	Volcanic and/or igneous body north of Filicudi Island
21	Igneous buried body between Sisifo and Marsili Smts.

A significant trend, SE-NW aligned, outlines a broad area located between the Vavilov and De Marchi seamounts. It includes a N-S elongated relief, corresponding to the Gortani ridge, and a region apparently without noticeable morphological structures, possibly indicating a deeper magnetic source of a probable igneous and basic nature. Similar features are evidenced by a SE-NW aligned well defined trend, including a region located NW of Stromboli Island and marked by a significant anomaly. This broad area does not correspond to any known structure and is not correlated with the topography, thus indicating the possible presence of a buried igneous body.

Analogously, the analytic signal evidenced: the presence of a volcanic and/or igneous body north of Filicudi Island, where a small volcanic edifice is known (Barberi *et al.*, 1991); a probable igneous buried body between Sisifo and Marsili Smts., below a relatively thick sedimentary cover recognised by Barberi *et al.* (1991).

An analytic signal anomaly appeared near the Cicerone Smt. (*cf.* Finetti and Del Ben, 1986; named Albatros Smt. in Barberi *et al.*, 1991). This submarine volcano, and another smaller structure nortwestward located of suspected volcanic nature, are outlined by an unique circular trend of maxima.

A probable correlation was also noted between a NW-SE aligned trend and two structures: the De Marchi Smt. and a secondary relief, possibly of volcanic nature (Barberi *et al.*, 1991). A large and intense analytic signal anomaly immediately south of the Asinara fault could be correlated, in its western side, to the Cornaglia Smt. and to another minor relief located northwestward. Its eastern side could be correlated to the Mayor Smt. (Barberi *et al.*, 1991) and, more doubtfully, to the Sallustio Smt. (Finetti and Del Ben, 1986). As about Cornaglia Smt. the high intensity of the analytic signal suggests the presence of igneous or volcanic rocks other than the sampled metapelites.

Immediately northward, the Baronie ridge is well outlined, on its western, southern and northeastern sides, whereas its other boundaries are more uncertain.

The presence of the Asinara fault (Finetti and Del Ben, 1986), even if not directly evidenced, can be inferred by the southward abrupt truncation of the N-S aligned tectonic line correlated to the Elba ridge. Similarly, some evidence of the right transcurrent Vulcano fault (Finetti and Del Ben, 1986) can be found. Another broad trend was located immediately south of Ponza Island and does not seem to correspond to any well defined structure previously recognized.

A noticeable anomaly allowed the formation of a circular maxima trend immediately south of the Cilento coastline. These maxima probably indicate the presence of a horst buried below young sediments.

Another structure, including Giglio Island (acid plutonites) and, northward, the «Formiche di Grosseto» reefs seems to be outlined by a number of maxima aligned in a N-S direction. However this correlation is uncertain because of the very low intensity of the analytic signal in the area.

The boundary analysis also recognized, even if not very clearly (due to data undersampling and to the very small extension of anomalies), the presence of several small structures located south of the Tuscanian Archipelago and west of the Tyrrhenian abyssal plain:

– A body located northwest of the Cassinis Smt. (11°30′-11°45′ Long. E and 40°40′-41° Lat. N.), doubtfully interpreted as volcanic centers (Barberi *et al.*, 1991).

– A body whose location has coordinates 12°05′ Long. E and 40°50′ Lat. N.

– Two bodies, doubtfully interpreted as volcanic centers (Barberi *et al.*, 1991), whose location has coordinates 10°55′ Long. E and 39°20′ Lat. N.

The nature of these latter structures, evidenced by small submarine hills, remains uncertain.

We have provided a rather extensive definition of the main structures by the boundary analysis in the Tyrrhenian Sea. Let us note, however, that some known structures such as Lucrezio, Orazio and Catullo (Finetti and Del Ben, 1986) and Secchi seamounts are poorly represented in the analytical signal map. Analogously for some minor ridges such as the Selli ridge or for tectonic lines like the Circeo, Capri, Tacito, Taormina and Filicudi faults (Finetti and Del Ben, 1986). This is mainly due to the regional type of utilized data, to interference between several neighboring anomalies or even to the fact that contacts with a low magnetization contrast are likely to generate weak anomalies, so that the maxima of the analytic signal are probably corrupted by the noise.

4. Conclusions

The techniques used here to study the Tyrrhenian region, based on the analysis of the horizontal gradient and of the analytic signal, are rather objective and proved to be very fast and efficient to yield an overall definition of and significant insights into the structures of the region. The method allowed a useful recognition of any kind of contacts between structures with a magnetization contrast. As a matter of fact, we found several previously known structures defining their lateral extent:

– Tectonic alignments: Elba ridge, Romolo line, Selli line, Ponza fault, Vulcano fault.

– On-shore volcanoes: Bolsena, Vico, Bracciano, Albano, Roccamonfina, Vesuvius, Phlegraean Fields, etc.

– Submarine volcanoes: Marsili, Vavilov, Anchise, Quirra, Enarete, Eolo and Sisifo Smts., etc.

– Submarine crystalline outcrops: Ichnusa, Vercelli, M. della Rondine, Tiberino, Cassinis, Traiano, Glauco and Augusto Smts., etc.

However, a more noticeable result was the identification of several trends indicating the existence of source bodies whose nature is still unknown or imperfect:

– A broad area located between the Vavilov and De Marchi seamounts.

– A region located NW of Stromboli Island.

– A volcanic and/or igneous body north of Filicudi Island.

– An igneous buried body between Sisifo and Marsili Smts.

– An area south of Ponza Island.

– A buried horst immediately south of the Cilento coastline.

– A body located northwest of the Cassinis Smt.

– Several small magnetized structures located south of the Tuscanian Archipelago, etc.

Some of them have small dimensions or are partially or totally buried by more recent sediments and, consequently, are not correlated to the bathimetry. Other sources (south of the Magnaghi Smt.; between the Vavilov and the De Marchi Smts.; northwest of the Stromboli Island) are more extended than what was inferred from the submarine reliefs associated to them.

Difficulties in distinguishing some local structures and the apparent sparseness of some maxima points, are mainly due to the regional character of the utilized aeromagnetic data set. The availability of more detailed input data could avoid these drawbacks and allow a more precise edge analysis also at a local scale.

Acknowledgements

This research was partially supported by grants MURST 40% 1995, 1996 and by grants CNR 1994, 1995, 1996.

REFERENCES

AGIP (1981): *Carta Aeromagnetica d'Italia* (scala 1:500 000), Att. Min., Direz. Espl. Idrocarburi, S. Donato Milanese.

BARANOV, V. (1975): *Potential Fields and their Transformation in Applied Geophysics* (Gebruder Borntraeger, Stuttgart), p. 121.

BARBERI, F., G. BIGI, A. CASTELLARIN, R. CATALANO, M. COLI, D. COSENTINO, G.V. DAL PIAZ, F. LENTINI, M. PAROTTO, E. PATACCA, A. PRATURLON, F. SALVINI, R. SARTORI, P. SCANDONE and G.B. VAI (1991): *Structural Model of Italy*, Progetto Finalizzato Geodinamica (CNR).

BARBIERI, M., G. GASPAROTTO, F. LUCCHINI, C. SAVELLI and L. VIGLIOTTI (1986): Contributo allo studio del magmatismo nel Mar Tirreno: l'intrusione granitica tardo-miocenica del monte submarino Vercelli, *Mem. Soc. Geol. It.*, **36**, 41-54.

BERNINI, M., M. BOCCALETTI, G. MORATTI, G. PAPANI, F. SANI and L. TORELLI (1990): Episodi compressivi neogenico-quaternari nell'area estensionale tirrenica Nord-Orientale. Dati in mare e a terra, *Mem. Soc. Geol. It.*, **45**, 577-589.

BLAKELY, R.J. and R.W. SIMPSON (1986): Approximating edges of source bodies from magnetic or gravity anomalies, *Geophysics*, **51** (7), 1494-1498.

CORDELL, L. (1979): Gravimetric expression of graben faulting in Santa Fe country and the Espanola basin, New Mexico, in *30th Field Conference, New Mexico Geol. Soc., Guidebook*, 59-64

CORDELL, L. and V.J.S. GRAUCH (1985): Mapping basement magnetization zones from aeromagnetic data in the San Juan basin, New Mexico, in *The Utility of Regional Gravity and Magnetic Anomaly Maps*, edited by W.J. HINZE (Soc. Explor. Geophys.), 181-197.

DOGLIONI, C. (1991): A proposal of kinematic modelling for W-dipping subductions – Possible applications to the Tyrrhenian-Appennines system, *Terra Nova*, **3**, 423-434.

DOGLIONI, C. and G. FLORES (1995): *An Introduction to the Italian Geology* (Ed. Il Salice, Potenza), p. 98.

FEDI, M. (1990): On the quantitative interpretation of magnetic anomalies by pseudo-gravimetric integration, *Terra Nova*, **1**, 564-572.

FEDI, M. and A. RAPOLLA (1988): Rotation of the Italian Peninsula from aeromagnetic evidence, *Phys. Earth Planet. Int.*, **52**, 301-307.

FEDI, M., G. FLORIO and A. RAPOLLA (1994): The Magnaghi seamount: a gravimetric and magnetic combined study, *Boll. Geofis. Teor. Appl.*, **36** (141-144), 523-531.

FINETTI, I. and A. DEL BEN (1986): Geophysical study of the Tyrrhenian opening, *Boll. Geofis. Teor. Appl.*, **28** (110), 75-155.

FLORIO, G. (1993): An interpretation of abnormally shaped magnetic anomalies in South-Eastern Italy, *Boll. Geofis. Teor. Appl.*, **35** (140), 447-461.

GRAUCH, V.J.S. and L. CORDELL (1987): Limitations of determining density or magnetic boundaries from the horizontal gradient of gravity or pseudogravity data, *Geophysics*, **52** (1), 118-121.

INCORONATO, A. and G. NARDI (1989): Palaeomagnetic evidences for a peri-Tyrrhenian orocline, in *The Lithosphere in Italy*, Accad. Naz. dei Lincei, 217-227.

KASTENS, K., J. MASCLE, C. AUROUX, E. BONATTI, C. BROGLIA, J.E.T. CHANNELL, P. CURZI, K.C. EMEIS, G. GLAÇON, S. HASEGAWA, W. HIEKE, G. MASCLE, F. MCCOY, J. MCKENZIE, J. MENDELSON, C. MÜLLER, J.P. RÉHAULT, A. ROBERTSON, R. SARTORI, R. SPROVIERI and M. TORII (1988): ODP Leg 107 in the Tyrrhenian Sea: insights into passive margin and back-arc basin evolution, *Bull. Amer. Geol. Soc.*, **100**, 1140-1156.

LOCARDI, E. and R. NICOLICH (1988): Geodinamica del Tirreno e dell'Appennino Centro-Meridionale: la nuova carta della Moho, *Mem. Soc. Geol. It.*, **41**, 121-140.

MALINVERNO, A. and W.B.F. RYAN (1986): Extension in Tyrrhenian Sea and shortening in the Appennines as a result of arc migration driven by sinking of the lithosphere, *Tectonics*, **5** (2), 227-245.

MORELLI, C. (1982): Le conoscenze geofisiche dell'Italia e mari antistanti, *Mem. Soc. Geol. It.*, **24**, 521-530.

MOUSSAT, E., J.P. RÉHAULT, A. FABBRI and G. MASCLE (1985): Evolution géologique de la mer Tyrrhénienne, *C. R. Acad. Sci.,* **301** (7), 491-496.

NABIGHIAN, M. (1984): Toward a three-dimensional automatic interpretation of potential field data via generalized Hilbert transforms: fundamental relations, *Geophysics*, **49** (49), 780-786.

PATACCA, E., R. SARTORI and P. SCANDONE (1990): Tyrrhenian basin and Appenninic arcs: kinematic relations since Late Tortonian times, *Mem. Soc. Geol. It.*, **45**, 453-462.

PEIRCE, C. and P.J. BARTON (1992): Southern segment of the European Geotraverse – A wide-angle seismic refraction experiment in the Sardinia Channel, *Mar. Geophys. Res.*, **14**, 227-248.

ROEST, W.R., J. VERHOEF and M. PILKINGTON (1992): Magnetic interpretation using the 3D analytic signal, *Geophysics*, **57** (1), 116-125.

SELLI, R. (1981): Thoughts on the geology of the Mediterranean region, in *Sedimentary Basins of Mediterranean Margins, Italian Project of Oceanography*, edited by F.C. WEZEL (Tecnoprint, Bologna), 489-501.